JOC Article

Photochemically Stable Fluorescent Heteroditopic Ligands for Zinc Ion

Lu Zhang and Lei Zhu*

Department of Chemistry and Biochemistry, Florida State University, Tallahassee, Florida 32306-4390

lzhu@chem.fsu.edu

Received July 10, 2008

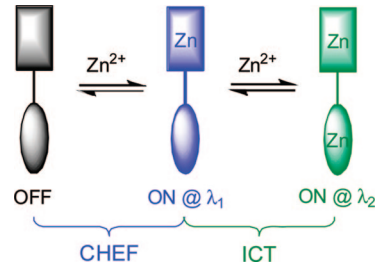

Photochemically stable fluorescent heteroditopic ligands (**9** and **10**) for zinc ion were prepared and studied. Two independent metal coordination-driven photophysical processes, chelation-enhanced fluorescence (CHEF) and internal (or intramolecular) charge transfer (ICT), were designed into our heteroditopic ligand framework. This strategy successfully relates three coordination states of a ligand, non-, mono-, and dicoordinated, to three fluorescence states, fluorescence OFF, ON at one wavelength, and ON at another wavelength. This ligand platform has provided chemical foundation for applications such as the quantification of zinc concentration over broad ranges (Zhang, L.; Clark, R. J.; Zhu, L. *Chem.−Eur. J.* 2008, *14*, 2894−2903) and molecular logic functions (Zhang, L.; Whitfield, W. A.; Zhu, L. *Chem. Commun.* 2008, 1880−1882). The binding stoichiometries of dipicolylamino and 2,2′-bipyridyl, the two binding sites featured in heteroditopic ligands **7**−**10**, were studied in acetonitrile using both Job's method of continuous variation and isothermal titration calorimetry (ITC). The fluorescence enhancement of **7**−**10** upon the formation of monozinc complexes (defined as the fluorescence quantum yield ratio of monozinc complex and free ligand) is qualitatively related to the highest occupied molecular orbital (HOMO) energy levels of their fluorophores. This is consistent with our hypothesis on the thermodynamics of the coordination-driven photophysical processes embodied in the designed heteroditopic system, which was supported by cyclic voltammetry studies. In conclusion, compounds **9** and **10** not only possess better photochemical stability but also display a higher degree of fluorescence turn-on upon formation of monozinc complexes than their vinyl counterparts **7** and **8**.

Introduction

The development of chemical systems whose properties (mechanical, optical, electronic, etc.) can be modulated through fast, reversible interactions (noncovalent or "dynamic" covalent[1]) with external chemical stimuli[2] is a major objective in the field of supramolecular chemistry.[3,4] These endeavors are envisaged to offer new tools such as sensors and machines within a nanometer size regime that cannot be developed via conventional, macroscopic manipulation of matter.[5−7] Equally important, the studies of supramolecular systems advance our understanding on the fundamental chemical and physical principles underlying their unique, often surprising stimulus-dependent properties.

A typical supramolecular system is heteroditopic metal coordination ligands that were first developed in the late 1970s[8]

(1) Rowan, S. J.; Cantrill, S. J.; Cousins, G. R. L.; Sanders, J. K. M.; Stoddart, J. F. *Angew. Chem., Int. Ed.* **2002**, *41*, 898–952.
(2) Feringa, B. L. *Molecular Switches*; Wiley-VCH: New York, 2001.
(3) Halpern, J. *Proc. Natl. Acad. Sci. U.S.A.* **2002**, *99*, 4762.
(4) Alper, J. *Science* **2002**, *295*, 2396–2397.
(5) Stoddart, J. F. *Acc. Chem. Res.* **2001**, *34*, 410–411.
(6) Balzani, V.; Venturi, M.; Credi, A. In *Molecular Devices and Machines - A Journey into the Nanoworld*; Wiley-VCH: Weinheim, 2003.
(7) Kay, E. R.; Leigh, D. A.; Zerbetto, F. *Angew. Chem., Int. Ed.* **2007**, *46*, 72–191.
(8) Rebek, J., Jr.; Trend, J. E.; Wattley, R. V.; Chakravorti, S. *J. Am. Chem. Soc.* **1979**, *101*, 4333–4337.

10.1021/jo8015083 CCC: $40.75
Published on Web 10/14/2008

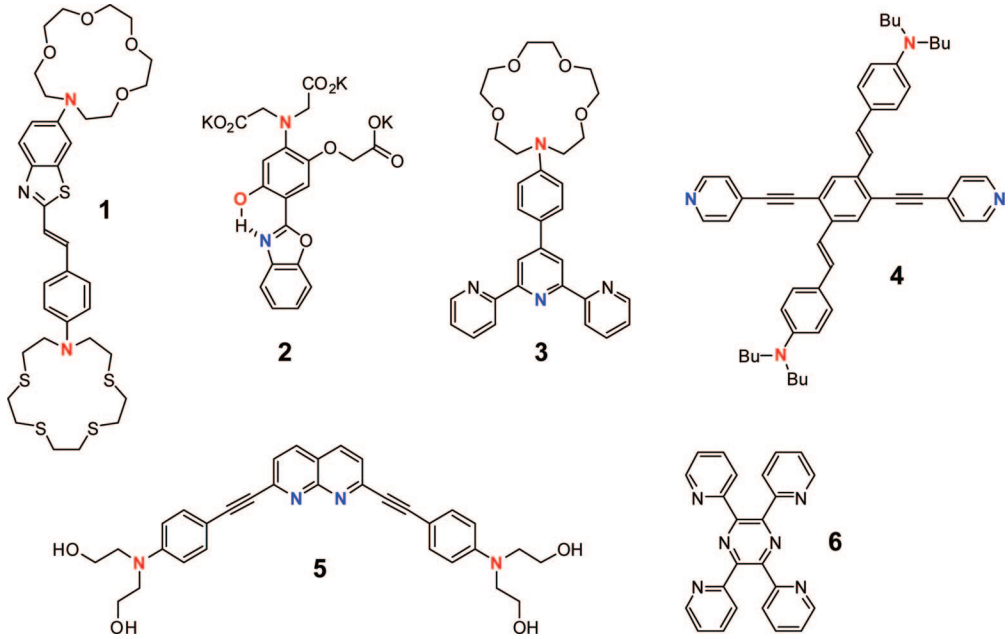

FIGURE 1. Compounds **1**−**4**: Fluorescent heteroditopic ligands for metal ions (refs 18−23). Red-coded atoms: electron donor sites; blue coded atoms: electron acceptor sites. **5**: A chromophoric ditopic ligand developed for Hg^{2+} sensing (ref 27). **6**: A fluorescent ligand capable of forming multinuclear complexes with Zn^{2+}, Sc^{3+}, and other metal ions (refs 28 and 29).

as model systems for allosterism found in Nature.[9] In this case, the external stimulus, a metal ion, is recognized by a metal coordination site (the "allosteric site") within the ditopic ligand. This interaction is transduced into a conformational change of the other metal coordination site (the "active site"), which is manifested as altered binding[10−15] and/or catalytic[16,17] properties of the "active site" of the heteroditopic ligand.

More recently, fluorescent ditopic ligands have been developed for transducing metal coordination events into fluorescence spectral shifts and/or intensity modulations.[18−23] On the basis of the identities and/or quantity of the metal ion present, a fluorescent ditopic ligand is capable of offering at least three coordination states, non-, mono-, and dicoordinated, which give rise to three distinct fluorescence states. Hence, fluorescent ditopic systems provide platforms for designing supramolecular systems to achieve practical goals that are unattainable via monotopic systems. Typical examples include the simultaneous detection of two different metal ions and imaging and quantification of a metal ion over large concentration ranges. The fundamental chemical challenge in all these applications is to achieve large fluorescence contrast of the three coordination states of a fluorescent ditopic ligand based on thorough understanding of its coordination-driven photophysical properties.

The coordination-modulated internal charge transfer (ICT)[24] and excited-state intramolecular proton transfer (ESIPT)[25,26] of donor−acceptor type fluorophores or chromophores have been a prominent theme in the development of fluorescent ditopic ligands with three different fluorescence states. Several examples are shown in Figure 1. The coordinating atoms that are critically impacting the fluorescence of the ligands are color-coded and bolded. The metal-coordination at the electron donor (red) and the electron acceptor (blue) atoms result in a hypsochromic and bathochromic shifts of emission, respectively.[24] Therefore, mono- and dicoordinated ligands have shorter or longer emission bands than that of the unbound ligand, depending on whether the donor or the acceptor atom is preferentially coordinated. The coordination-modulated ICT or ESIPT has been applied to achieve three fluorescence states in compounds **2**−**4**. The fluorophore of **1** does not have strong donor−acceptor characteristics; therefore, only small spectral shifts were observed when Ag^{+} and Na^{+} were introduced in the system.[18] The three coordination states of **5** achieved upon coordinating Hg^{2+} have distinct absorption bands.[27] However, their fluorescence properties were not reported. Although not a typical ditopic ligand, the ability of **6** to form multinuclear complexes with different photophysical properties was explored to achieve the same objective.[28,29]

(9) Kobe, B.; Kemp, B. E. *Nature* **1999**, *402*, 373–376.
(10) Rebek, J., Jr.; Wattley, R. V. *J. Am. Chem. Soc.* **1980**, *102*, 4853–4854.
(11) Rebek, J., Jr.; Marshall, L. *J. Am. Chem. Soc.* **1983**, *105*, 6668–6670.
(12) Nabeshima, T.; Yoshihira, Y.; Saiki, T.; Akine, S.; Horn, E. *J. Am. Chem. Soc.* **2003**, *125*, 28–29.
(13) Baylies, C. J.; Harding, L. P.; Jeffery, J. C.; Riis-Johannessen, T.; Rice, C. R. *Angew. Chem., Int. Ed.* **2004**, *2004*, 4515–4518.
(14) Akine, S.; Taniguchi, T.; Saiki, T.; Nabeshima, T. *J. Am. Chem. Soc.* **2005**, *127*, 540–541.
(15) Baylies, C. J.; Riis-Johannessen, T.; Harding, L. P.; Jeffery, J. C.; Moon, R.; Rice, C. R.; Whitehead, M. *Angew. Chem., Int. Ed.* **2005**, *44*, 6909–6912.
(16) Rebek, J., Jr.; Costello, T.; Wattley, R. V. *J. Am. Chem. Soc.* **1985**, *107*, 7487–7493.
(17) McSkimming, G.; Tucker, J. H. R.; Bouas-Laurent, H.; Desvergne, J.-P. *Angew. Chem., Int. Ed.* **2000**, *39*, 2167–2169.
(18) Rurack, K.; Koval'chuck, A.; Bricks, J. L.; Slominskii, J. L. *J. Am. Chem. Soc.* **2001**, *123*, 6205–6206.
(19) Ohshima, A.; Momotake, A.; Arai, T. *Tetrahedron Lett.* **2004**, *45*, 9377–9381.
(20) Ohshima, A.; Momotake, A.; Arai, T. *Sci. Tech. Adv. Mat.* **2005**, *6*, 633–643.
(21) Li, Y. Q.; Bricks, J. L.; Resch-Genger, U.; Spieles, M.; Rettig, W. *J. Phys. Chem. A* **2006**, *110*, 10972–10984.
(22) Wilson, J. N.; Bunz, U. H. F. *J. Am. Chem. Soc.* **2005**, *127*, 4124–4125.
(23) Zucchero, A. J.; Wilson, J. N.; Bunz, U. H. F. *J. Am. Chem. Soc.* **2006**, *128*, 11872–11881.
(24) Valeur, B.; Leray, I. *Coord. Chem. Rev.* **2000**, *205*, 3–40.
(25) Henary, M. M.; Fahrni, C. J. *J. Phys. Chem. A* **2002**, *106*, 5210–5220.
(26) Henary, M. M.; Wu, Y.; Fahrni, C. J. *Chem.−Eur. J.* **2004**, *10*, 3015–3025.
(27) Huang, J.-H.; Wen, W.-H.; Sun, Y.-Y.; Chou, P.-T.; Fang, J.-M. *J. Org. Chem.* **2005**, *70*, 5827–5832.

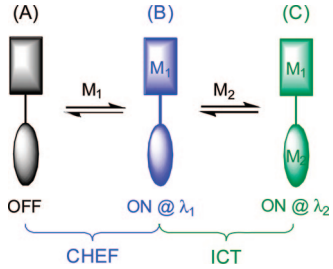

FIGURE 2. Three coordination states (non-, mono-, and dicoordinated) of a fluorescent heteroditopic ligand are related to three fluorescence states (OFF, ON at λ_1, and ON at λ_2). M1 and M2, two metal ions; CHEF, chelation-enhanced fluorescence; ICT, internal (or intramolecular) charge transfer.

These early examples advanced our understanding of fluorescent heteroditopic ligands; however accomplishing three different fluorescence states with large contrast is anything but trivial. Spectral shift was not observed in compounds **1** and **6** due to their inherently weak donor−acceptor characteristics. The coordination of compounds **2**−**4** resulted in fluorescence states with three different emission wavelengths for each ligand based on the rationale articulated earlier. However, one empirical, under-controlled factor is that metal coordination may open up extra or close existing nonradiative pathways, thus changing fluorescence intensity in a rather unpredictable manner. Therefore, we seek another design strategy so that control over both fluorescence intensity and spectral shift can be achieved to afford three fluorescence states with maximal contrast.

Our group is interested in developing fluorescence probes for zinc ion (Zn^{2+}) quantification and imaging with low detection limit, high sensitivity, and large effective concentration ranges.[30−32] We explore the heteroditopic platform to achieve the coverage of large concentration ranges in Zn^{2+} quantification applications.[32] In our work, two coordination-driven photophysical processes, chelation-enhanced fluorescence (CHEF) and coordination-modulated internal (or intramolecular) charge transfer (ICT), were engineered into a compact heteroditopic ligand framework for achieving three distinct coordination-dependent fluorescence states (Figure 2). The ligand itself was designed to have a nonradiative relaxation pathway where photoinduced electron transfer (PET) occurs from the electron-rich, high-affinity (the rectangles in Figure 2) Zn^{2+}-binding moiety to the excited fluorophore. Preferential coordination of Zn^{2+} to the high-affinity binding site raises its oxidation potential so that the PET process becomes thermodynamically disfavored. Consequently, the fluorescence is restored. This coordination-driven process has been referred to as chelation-enhanced fluorescence (CHEF).[33,34]

As the concentration of Zn^{2+} ([Zn]) is high enough to occupy the low-affinity site (the ovals in Figure 2), a charge-transferred, dipolar excited state (ICT state) of the ditopic ligand is expected to be stabilized (in the system reported in this paper) to result in a bathochromic shift of emission.[24] In summary, depending on the metal ion concentration, the non-, mono, and dicoordinated ligands adopt three fluorescence states—fluorescence OFF (Figure 2A), ON at one wavelength (Figure 2B), and ON at another wavelength (Figure 2C). State "A" has low fluorescence quantum yield (Φ_F) due to PET; States "B" and "C" can be designed to have large, comparable Φ_F, however they fluoresce at different wavelengths. On the basis of this unique ligand platform, applications such as metal ion quantification over large concentration ranges[32] and development of molecular logic functions[35] can be achieved (for overviews of the molecular logic area see refs 6 and 36−40).

In implementing this design, a series of fluoroionophores for Zn^{2+} with moderate affinities which are capable of Zn^{2+}-coordination modulated ICT will be studied first. The ligands with high fluorescence quantum yields in *both* free *and* Zn^{2+}-bound forms will be selected for installation of a PET/CHEF switching unit, which is also designed as the high-affinity Zn^{2+}-binding moiety. The theoretical ground for the choice of the PET/CHEF switch to achieve sensitive fluorescence turn-on upon coordinating Zn^{2+} will be detailed in the section of "Cyclic Voltammetry Studies". In summary, two independent coordination-driven photophysical processes (CHEF and ICT) are incorporated in one heteroditopic ligand framework. The sequential activation of CHEF and ICT processes is controlled by the relative affinities of the two Zn^{2+}-binding moieties associated with respective processes. By applying this design principle, control over both emission wavelengths and quantum yields of the three coordination-dependent fluorescence states of a fluorescent heteroditopic ligand can be accomplished.

A fluorescent heteroditopic ligand platform for Zn^{2+}, represented by compounds **7** and **8**, has been developed in our laboratory based on this design principle.[32] In the absence of Zn^{2+}, **7** and **8** are only weakly fluorescent (see Φ_F values in Table 1) because nonradiative relaxation via PET from the tertiary amino group in either **7** or **8** to the excited arylvinyl-bipy (bipy = 2,2′-bipyridyl) fluorophore is operating.[41] In the presence of Zn^{2+} at low concentration, preferential coordination to the presumptive high-affinity dipicolylamino group occurs to result in CHEF. When the concentration of Zn^{2+} is high enough to bind bipy, the presumptive low-affinity binding site, the charge-transferred excited fluorophore is stabilized to result in a bathochromic shift of the emission band.

Although the rational design of **7** and **8** is satisfactory, we seek to further expand the scope and practicality of our design of fluorescent heteroditopic ligands by fully understanding the fundamental coordination chemistry and photophysical processes embodied in this system. Herein, we report our progress in (1) preparing fluorescent heteroditopic systems that are photochemically stable, (2) studying the binding stoichiometries and relative affinities of dipicolylamino and bipy, which are the two binding motifs in this series of heteroditopic ligands (**7**−**10**), to Zn^{2+}, and (3) achieving large fluorescence contrasts between the three fluorescence states upon further understanding of the thermodynamics of the electron transfer processes.

(28) Yuasa, J.; Fukuzumi, S. *J. Am. Chem. Soc.* **2006**, *128*, 15976–15977.
(29) Yuasa, J.; Fukuzumi, S. *J. Am. Chem. Soc.* **2008**, *130*, 566–575.
(30) Zhang, L.; Dong, S.; Zhu, L. *Chem. Commun.* **2007**, 1891–1893.
(31) Huang, S.; Clark, R. J.; Zhu, L. *Org. Lett.* **2007**, *9*, 4999–5002.
(32) Zhang, L.; Clark, R. J.; Zhu, L. *Chem.−Eur. J.* **2008**, *14*, 2894–2903.
(33) Huston, M. E.; Haider, K. W.; Czarnik, A. W. *J. Am. Chem. Soc.* **1988**, *110*, 4460–4462.
(34) Akkaya, E. U.; Huston, M. E.; Czarnik, A. W. *J. Am. Chem. Soc.* **1990**, *112*, 3590–3593.
(35) Zhang, L.; Whitfield, W. A.; Zhu, L. *Chem. Commun.* **2008**, 1880–1882.
(36) Brown, G. J.; de Silva, A. P.; Pagliari, S. *Chem. Commun.* **2002**, 2461–2463.
(37) de Silva, A. P.; McClenaghan, N. D. *Chem.−Eur. J.* **2004**, *10*, 574–586.
(38) de Silva, A. P.; Uchiyama, S. *Nat. Nanotechnol.* **2007**, *2*, 399–410.
(39) Magri, D. C.; Vance, T. P.; de Silva, A. P. *Inorg. Chim. Acta* **2007**, *360*, 751–764.
(40) Pischel, U. *Angew. Chem., Int. Ed.* **2007**, *46*, 4026–4040.
(41) de Silva, A. P.; Gunaratne, H. Q. N.; Gunnlaugsson, T.; Huxley, A. J. M.; McCoy, C. P.; Rademacher, J. T.; Rice, T. E. *Chem. Rev.* **1997**, *97*, 1515–1566.

TABLE 1. Fluorescence Quantum Yields of Free Ligands (Φ_F), Monozinc Complex (Φ_{ZnL}), and Dizinc Complex (Φ_{Zn2L}), Emission Band Maxima (λ_1, λ_2) of Ligands and Their Zn^{2+} Complexes, and Anodic Peak Potentials of the Free Ligands in MeCN

	Φ_F	Φ_{ZnL}	Φ_{ZnL}/Φ_F	Φ_{Zn2L}	λ_1/nm	λ_2/nm	(λ_2-λ_1)/nm	E_{pa}/mV
7	0.024 ± 0.0008	0.35[a]	15	0.70 ± 0.01	392[b]	454[b]	62	1636, 1114
8	0.038 ± 0.001	0.095[a]	2.5	0.32 ± 0.007	419[b]	496[b]	77	1385, 1161
9	0.0087 ± 0.0006	0.29[a]	33	0.63 ± 0.035	367	415	48	1890, 1120
10	0.0092 ± 0.001	0.046[a]	5.0	0.074 ± 0.0025	392	472	80	1698, 1178
11	0.51 ± 0.02	0.67 ± 0.006	1.3	N. A.	392	459	67	1567 ± 4
12	0.039 ± 0.002	0.26 ± 0.02	6.7	N. A.	423[b]	504[b]	81	1356 ± 14
13	0.20 ± 0.002	0.81 ± 0.025	4.0	N. A.	364	420	56	1886 ± 6
14	0.014 ± 0.0006	0.042 ± 0.0012	3.0	N. A.	390	480	90	1660 ± 4

[a] The monozinc complex of a heteroditopic ligand is considered as the species with ligand:zinc ratio that maximizes the shorter emission band (at λ_1). The Φ_F was determined using the corresponding free ligand as the reference. [b] Data were taken from ref 32.

Structures

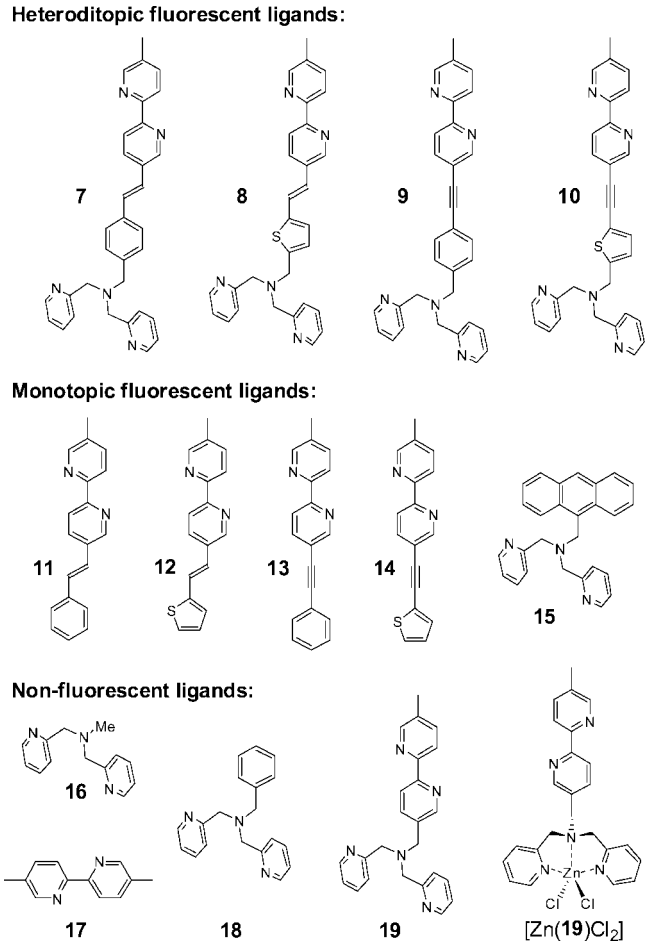

Results and Discussion

Compounds **7** and **8** undergo *trans* → *cis* photoisomerization readily upon ambient irradiation (Figure 3). Furthermore, stilbenoid structures such as **7** and **8** are known to have different emissive conformers in their excited states,[42−45] which may complicate the later data analysis. A conservative chemical modification which replaces the isomerizable double bonds with triple bonds was envisioned to afford photochemically stable **9** and **10** while maintaining the coordination-driven fluorescence switching functions of **7** and **8**.[46]

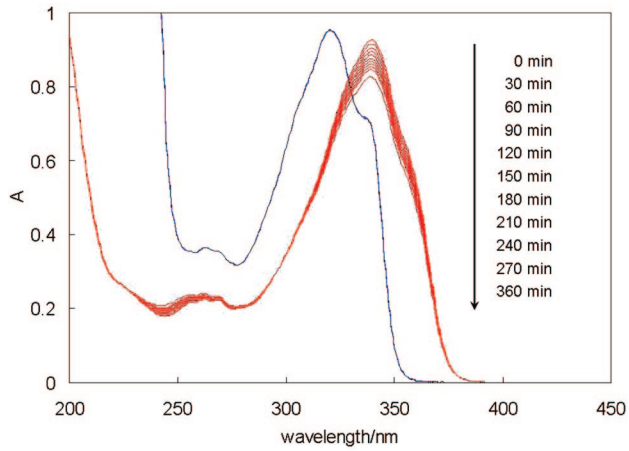

FIGURE 3. Absorption spectra of **7** (red, 20 μM) and **9** (blue, 20 μM) in MeCN. Samples were exposed to ambient light. The absorption spectra were collected every 30 min.

Synthesis. The synthesis of **9** is shown in Scheme 1. Radical bromination of 5,5′-dimethyl-2,2′-dipyridyl (**17**) with 1 equiv NBS followed immediately (without purification) with an Arbuzov phosphonate synthesis afforded **20**. Phosphonate **20** was easily isolatable, in contrast to its monobrominated precursor, in 48% yield over two steps. The Horner−Wadsworth−Emmons reaction between **20** and **21** gave **22**, which underwent a two-step sequence of dibromination−didehydrobromination[47−49] to afford alkyne **23**. Upon acidic deprotection, reductive amination between **24** and di-(2-picolyl)amine gave rise to compound **9** to complete an overall efficient synthesis. The syntheses and characterizations of other new compounds are described in the Supporting Information.

Photochemical Stability. Under ambient irradiation over 6 h, the absorption spectrum of alkynyl compound **9** did not change while the absorption band centered at 339 nm of vinyl compound **7** decreased readily over time (Figure 3), characteristic of a *trans*→*cis* photoisomerization.[50] Compound **8** isomerized more readily than **7** as shown by absorption scans and ^{1}H NMR

(42) Mazzucato, U.; Momicchioli, F. *Chem. Rev.* **1991**, *91*, 1679–1719.
(43) Saltiel, J.; Tarkalanov, N.; Sears, D. F., Jr. *J. Am. Chem. Soc.* **1995**, *117*, 5586–5587.
(44) Saltiel, J.; Zhang, Y.; Sears, D. F., Jr. *J. Am. Chem. Soc.* **1997**, *119*, 11202–11210.
(45) Alfimov, M. V.; Gromov, S. P.; Fedorov, Y. V.; Fedorova, O. A.; Vedernikov, A. I.; Churakov, A. V.; Kuz'mina, L. G.; Howard, J. A. K.; Bossmann, S.; Braun, A.; Woerner, M.; Sears, D. F., Jr.; Saltiel, J. *J. Am. Chem. Soc.* **1999**, *121*, 4992–5000.
(46) Benniston, A. C.; Harriman, A.; Grosshenny, V.; Ziessel, R. *New J. Chem.* **1997**, *21*, 405–408.
(47) Cava, M. P.; Pohlke, R.; Erickson, B. W.; Rose, J. C.; Fraenkel, G. *Tetrahedron* **1962**, *18*, 1005–1011.
(48) Wong, H. N. C.; Garratt, P. J.; Sondheimer, F. *J. Am. Chem. Soc.* **1974**, *96*, 5604–5605.
(49) Wilcox, C. F. J.; Weber, K. A. *J. Org. Chem.* **1986**, *51*, 1088–1094.

SCHEME 1[a]

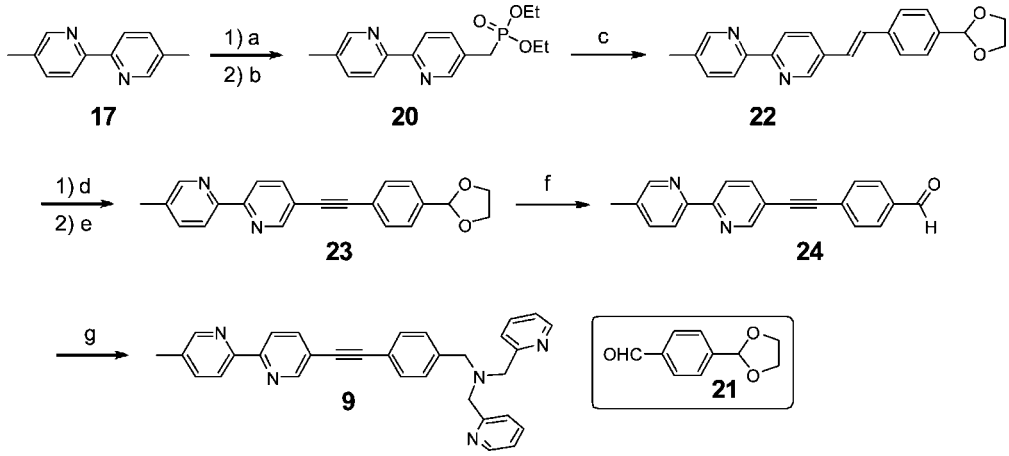

[a] (a) NBS, AIBN (cat.), CCl_4, reflux, 2.5 h; (b) $(EtO)_3P$, 125 °C, 3 h, 48%, two steps; (c) **21**, NaH, rt, 4 h, 75%; (d) Br_2, DCM, rt, 3 h; (e) tBuOK, THF, rt, 14 h, 25%, two steps; (f) HCl/H_2O/THF, rt, 14 h; (g) di-(2-picolyl)amine, $NaBH(OAc)_3$, rt, 6 h, 73%, two steps.

(Supporting Information), presumably due to its larger molar absorptivity in the visible spectrum than that of **7**.

Absorption and Fluorescence Titration Studies. The Zn^{2+} titration experiments of compounds **9** and **10** were carried out in MeCN. The absorption and fluorescence spectra at different Zn^{2+} concentrations ([Zn]) were collected (Figures 4 and 5, binding isotherms in the Supporting Information). Both ligands display weak fluorescence (blue spectra) in their free forms due to PET from the tertiary nitrogen atoms to the excited arylalkynyl-bipy fluorophores. Upon increasing [Zn], fluorescence intensity of both compounds are greatly enhanced, presumably due to CHEF, followed by bathochromic shifts of emission bands as the [Zn] is high enough to coordinate with bipy. The experiments that independently verified the sequential coordination of Zn^{2+} by heteroditopic ligands **7**−**10** in solution will be presented in the section of "Binding Studies". The overall fluorescence responses of **9** and **10** to Zn^{2+} are similar to those of **7** and **8**;[32] however, the fluorescence enhancements upon coordinating the first Zn^{2+} by **9** and **10** are much greater than those of **7** and **8**. The enhanced sensitivity in fluorescence turn-on of **9** and **10** upon binding the first Zn^{2+} is expected to expend the utility of this heteroditopic system in various applications.

Fluorescence Quantum Yield Measurements. The fluorescence quantum yields (Φ_F) of free ligands **7**−**14** and the dizinc complexes of **7**−**10** were measured by a relative method using either 2-aminopyridine or quinine bisulfate in 0.05 M sulfuric acid as references.[51] The dizinc samples were prepared using 2 μM of the respective ligands and 6 or 10 equiv of zinc so that full saturations of the ligands as dizinc complexes were ensured based on the binding isotherms of **7**−**10**.

The Φ_F measurements of monozinc complexes of **7**−**10** required special considerations. A solution sample containing only monozinc species cannot be prepared by using equal molar of a heteroditopic ligand and Zn^{2+} due to competitive equilibria with the free ligand and the dizinc complex (Figure 2). Furthermore, the species distribution at equal molar of ligand and Zn^{2+} is expected to be dependent on the concentration of the ligand. At a fixed ligand concentration (e.g., 2 μM), the emission intensity and band profile (shape and position) are highly sensitive to [Zn] when the ratio of ligand and Zn^{2+} is close to 1:1. The measured Φ_F values varied greatly with only minimal standard deviation of [Zn]. Therefore, it became clear

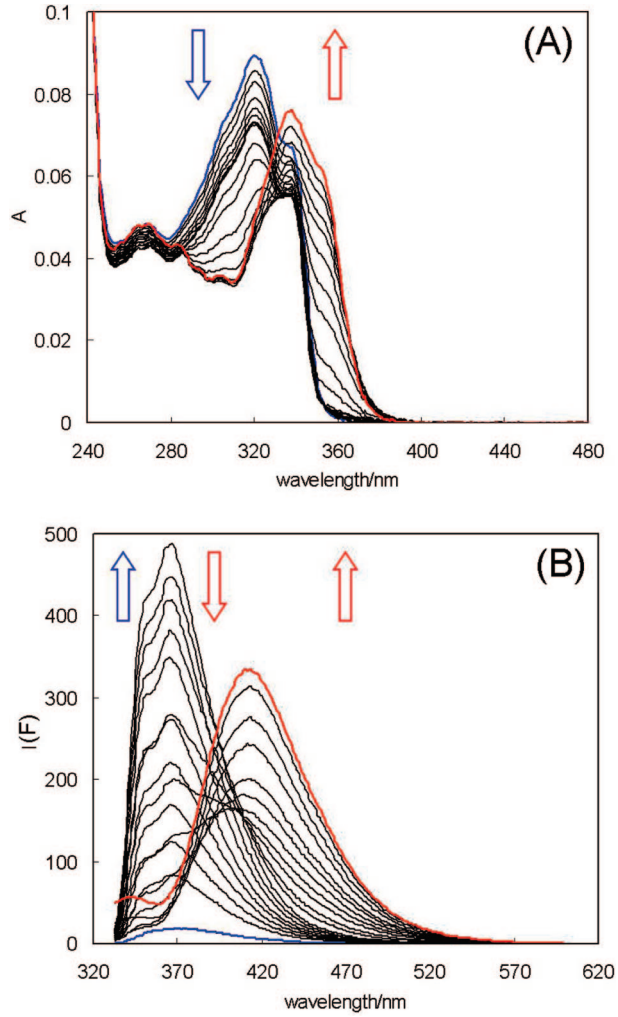

FIGURE 4. Absorption (A) and fluorescence (B, λ_{ex} = 321 nm) spectra of **9** (2.0 μM) in MeCN (TBAP: 5 mM; DIPEA: 2.0 μM; DMSO: 0.1%) upon addition of $Zn(ClO_4)_2$ (0−7.9 μM and 0−8.8 μM, respectively). The blue arrows represent the initial spectral changes; the red arrows represent the following bathochromic shifts. Blue spectra were taken in the absence of Zn^{2+}; the red spectra were taken in the presence of 7.9 μM (A) and 8.8 μM (B), respectively, of Zn^{2+}.

(50) Kopecky, J. *Organic Photochemistry: A Visual Approach*; VCH Publishers, Inc.: New York, 1992.
(51) Fery-Forgues, S.; Lavabre, D. *J. Chem. Educ.* **1999**, *76*, 1260–1264.

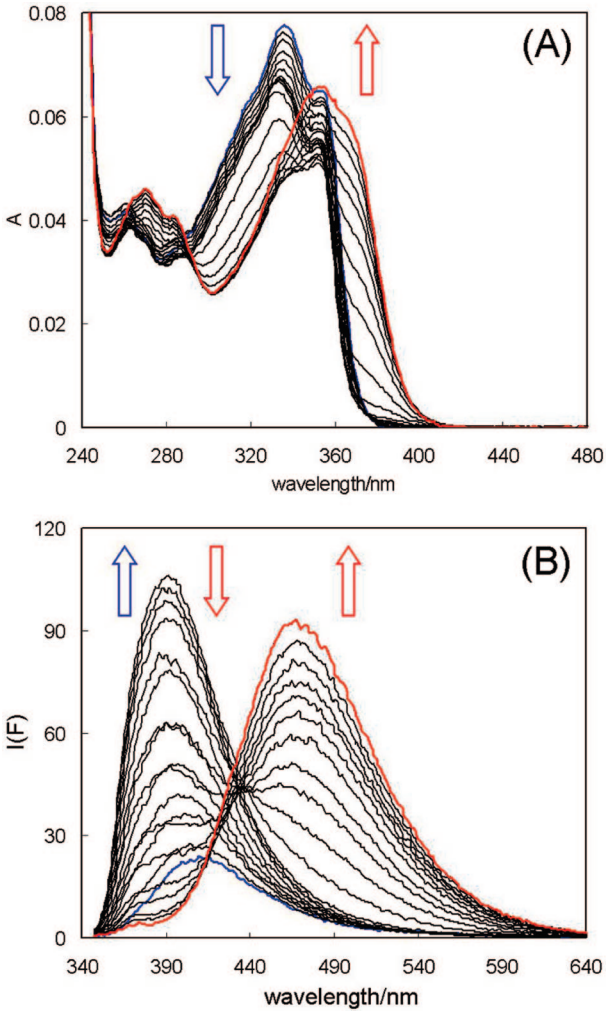

FIGURE 5. Absorption (A) and fluorescence (B, λ_{ex} = 335 nm) spectra of **10** (2.0 μM) in MeCN (TBAP: 5 mM; DIPEA: 2.0 μM; DMSO: 0.1%) upon addition of $Zn(ClO_4)_2$ (0−7.9 μM and 0−8.8 μM, respectively). The blue arrows represent the initial spectral changes; the red arrows represent the following bathochromic shifts. Blue spectra were taken in the absence of Zn^{2+}; the red spectra were taken in the presence of 7.9 μM (A) and 8.8 μM (B), respectively, of Zn^{2+}.

to us that determination of Φ_F of a monozinc complex using a sample of equal molar ligand and Zn^{2+} not only does not reflect the Φ_F of the monozinc complex as a unimolecular entity, but also gives rise to poor reproducibility. In light of those observations, we decided that the Φ_F of a monozinc complex was best represented as the Φ_F of the sample that gave rise to the highest fluorescence intensity at the shorter emission wavelength. In this case, the free ligand was used as the reference.

The emission wavelengths and fluorescence quantum yields of **7**−**14** and their zinc complexes are compiled in Table 1. The two parameters Φ_{ZnL}/Φ_F and $\Delta\lambda$ ($\lambda_1-\lambda_2$), representing fluorescence enhancement upon first Zn^{2+} coordination and emission spectral shift upon second Zn^{2+} coordination, define the "fluorescence contrast" of the three coordination states of a heteroditopic ligand. The benzene-derived **7** and **9** achieved much higher fluorescence turn-on upon coordinating the first Zn^{2+} as evidenced by large Φ_{ZnL}/Φ_F values (15 and 33, respectively) than the thiophene-derived **8** and **10**. The fluorescence quantum yields of both free ligands and monozinc complexes of **8** and **10** are low (<0.1), suggesting that there

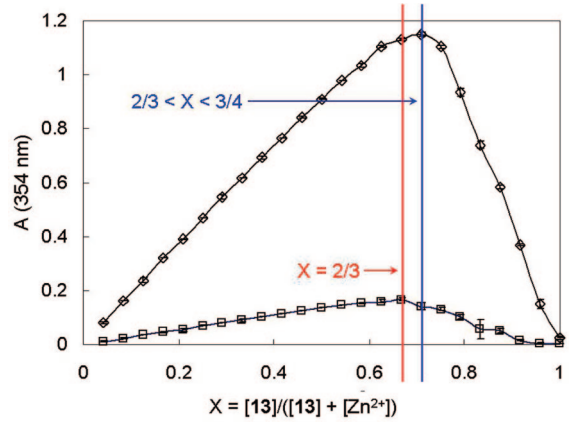

FIGURE 6. Job plots of association between **13** and $Zn(ClO_4)_2$ in MeCN. The total molar concentrations of **13** and $Zn(ClO_4)_2$ are 10 μM (□) and 60 μM (◇). The mole fraction (X) of **13** was varied continuously from 0 to 1.

are other nonradiative pathways available than photoinduced electron transfer in the free ligands. On the other hand, **8** and **10** display slightly larger emission spectral shift upon coordinating the second Zn^{2+} than the benzene-derived **7** and **9**; presumably because thiophene is a stronger electron-donor than benzene to afford more efficient internal charge transfer characters in the excited states of **8** and **10** (also in **12** and **14**). Based on the data collected in acetonitrile, we conclude that the overall fluorescence contrasts between different coordination states of **7** and **9** are better suited for the design outlined in Figure 2, where a large fluorescence turn-on upon the first Zn^{2+} coordination and a large emission spectral shift upon the second Zn^{2+} coordination are desired. To our knowledge, this is the first time that such large fluorescence contrast of three coordination states of a heteroditopic ligand has been reported. Studies of these ligands in other media are in progress.

Binding Studies. The conversion from vinyl to alkynyl substituents does not appear to affect the affinity of substituted bipy to Zn^{2+} under the conditions used in our studies, as supported by the almost overlapping spectrophotometric binding isotherms of **12** and **14** (Figure S10, Supporting Information).

In the previous study,[32] the preferential coordination of dipicolylamino over bipy to Zn^{2+} in MeCN was inferred from the X-ray single crystal structure of a mono-Zn^{2+} complex ([Zn(**19**)Cl_2] of a model ditopic ligand (**19**). The apparent association constants extracted from the binding isotherms using a 1:1 model supported that dipicolylamino group binds Zn^{2+} stronger than bipy.[32] However, the relatively small difference (within 1 order of magnitude) observed in the previous study prompted us to examine the binding of dipicolylamino and bipy to Zn^{2+} in MeCN in more detail.

In this study, the binding stoichiometry between bipy and Zn^{2+} was investigated first. A number of studies using 2,2′-bipy-based fluorescent ligands as Zn^{2+} sensors reported 1:1 binding stoichiometry;[52−55] other work suggested 2:1 or 3:1 (ligand:Zn^{2+}) stoichiometry.[56,57] In our study, Job's method of

(52) Ajayaghosh, A.; Carol, P.; Sreejith, S. *J. Am. Chem. Soc.* **2005**, *127*, 14962–14963.
(53) Dennis, A. E.; Smith, R. C. *Chem. Commun.* **2007**, 4641–4643.
(54) Leroy, S.; Soujanya, T.; Fages, F. *Tetrahedron Lett.* **2001**, *42*, 1665–1667.
(55) Leroy-Lhez, S.; Allain, M.; Oberle, J.; Fages, F. *New J. Chem.* **2007**, *31*, 1013–1021.
(56) Bilyk, A.; Harding, M. M.; Turner, P.; Hambley, T. W. *J. Chem. Soc., Dalton Trans.* **1994**, 2783–2790.

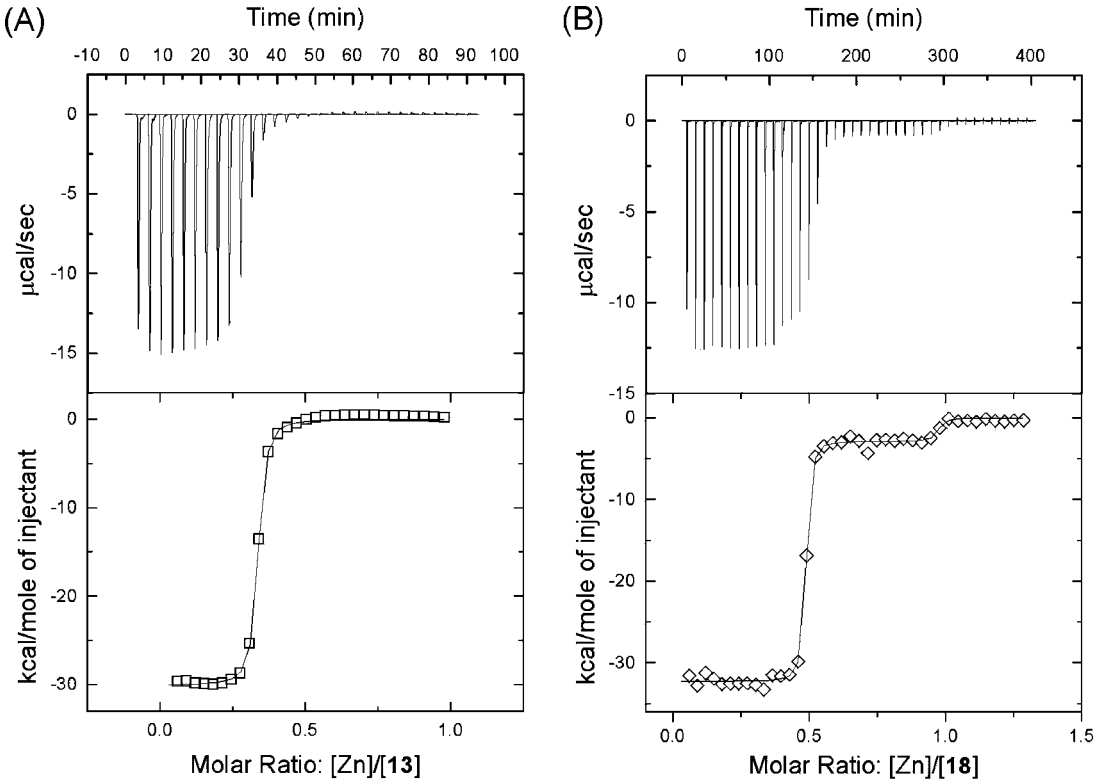

FIGURE 7. ITC data of (A) a 3:1 (**13**:Zn^{2+}) association ($n = 0.345$, $\Delta H° = -29.96$ kcal/mol) and (B) a two-step (**18**:Zn^{2+}) association ($n_1 = 0.474$, $\Delta H°(1) = -32.26$ kcal/mol; $n_2 = 0.484$, $\Delta H°(2) = -2.839$ kcal/mol) in MeCN at 298 K.

continuous variation[58] (Figure 6) revealed a 2:1 binding stoichiometry between **13** and Zn^{2+} at a total concentration of 10 μM ([**13**] + [Zn]). However, when the total concentration was increased to 60 μM, the binding stoichiometry shifted toward 3:1 (**13**:Zn^{2+}). To study the binding stoichiometry at higher concentrations, isothermal titration calorimetry (ITC) was applied.

Traditionally used for the determination of binding enthalpy ($\Delta H°$), free energy ($\Delta G°$), entropy ($\Delta S°$), and stoichiometry (n) of protein-receptor interactions,[59−62] isothermal titration calorimetry (ITC) has become increasingly important in studying supramolecular systems.[63−69] However, the examples of using ITC in studying metal−ligand coordination *in organic solvents* are rare,[70,71] partly because $\Delta G°$ of metal coordination in organic solvents is usually larger than what may be accurately measured by ITC. However, we note that the $\Delta H°$ and n values can still be reliably determined from ITC experiments.[59,70]

The ITC study of the association between **13** and Zn^{2+} revealed a 3:1 (**13**:Zn^{2+}) stoichiometry when [**13**] is 300 μM (Figure 7A). Combining with the results from the Job's plots, it is evident that the binding stoichiometry between bipy and Zn^{2+} is concentration-dependent: high concentration favors 3:1 stoichiometry, same as that observed between **17** and Zn^{2+} (Supporting Information), while at low concentration, 2:1 and 1:1 associations become feasible. Other factors that impact binding stoichiometry between bipy derivatives and transition metals are solvent, counterions, and substituent groups as suggested by other studies.[53]

Contrary to a simple 1:1 binding in MeCN reported in literature,[72] the titration of dipicolylamino group (represented by **18**) with Zn^{2+} in MeCN shows two calorimetrically distinct processes (Figure 7B), suggesting 2:1 (**18**:Zn^{2+}) binding followed by breaking off the 2:1 complex to a 1:1 complex as [Zn]/[**18**] increases.[70,71] Our study suggests that caution be applied when binding stoichiometry is interpreted using either Job's method or ITC alone. A full account on the studies of binding stoichiometry between polydentate ligands and Zn^{2+} using both ITC and Job plots will be reported at a later time.

A competitive binding experiment between **14** and **15** was carried out for demonstrating the difference in affinity between the dipicolylamino group and bipy in MeCN. As shown in Figure 8, the addition of Zn^{2+} in a solution of **14** and **15** at 2

(57) Senechal, K.; Maury, O.; Le Bozec, H.; Ledoux, I.; Zyss, J. *J. Am. Chem. Soc.* **2002**, *124*, 4560–4561.
(58) Connors, K. A. *Binding Constants, The Measurement of Molecular Complex Stability*; John Wiley and Sons: New York, 1987.
(59) Wiseman, T.; Williston, S.; Brandts, J. F.; Lin, L.-N. *Anal. Biochem.* **1989**, *179*, 131–137.
(60) Freire, E.; Mayorga, O. L.; Straume, M. *Anal. Chem.* **1990**, *62*, 950A–959A.
(61) Ladbury, J. E.; Chowdhry, B. Z. *Chem. Biol.* **1996**, *3*, 791–801.
(62) Wadso, I. *Chem. Soc. Rev.* **1997**, 79–86.
(63) Berger, M.; Schmidtchen, F. P. *Angew. Chem., Int. Ed.* **1998**, *37*, 2694–2696.
(64) Haj-Zaroubi, M.; Mitzel, N. W.; Schmidtchen, F. P. *Angew. Chem., Int. Ed.* **2002**, *41*, 104–107.
(65) Schmidtchen, F. P. *Org. Lett.* **2002**, *4*, 431–434.
(66) Otto, S.; Kubik, S. *J. Am. Chem. Soc.* **2003**, *125*, 7804–7805.
(67) Haj-Zaroubi, M.; Schmidtchen, F. P. *ChemPhysChem* **2005**, *6*, 1181–1186.
(68) Sessler, J. L.; Gross, D. E.; Cho, W.-S.; Lynch, V. M.; Schmidtchen, F. P.; Bates, G. W.; Light, M. E.; Gale, P. A. *J. Am. Chem. Soc.* **2006**, *128*, 12281–12288.
(69) Jadhav, V. D.; Schmidtchen, F. P. *J. Org. Chem.* **2008**, *73*, 1077–1087.
(70) Dobrawa, R.; Lysetska, M.; Ballester, P.; Grune, M.; Wurthner, F. *Macromolecules* **2005**, *38*, 1315–1325.
(71) Shunmugam, R.; Gabriel, G. J.; Smith, C. E.; Aamer, K. A.; Tew, G. N. *Chem.−Eur. J.* **2008**, *14*, 3904–3907.
(72) de Silva, S. A.; Zavaleta, A.; Baron, D. E.; Allam, O.; Isidor, E. V.; Kashimura, N.; Percapio, J. M. *Tetrahedron Lett.* **1997**, *38*, 2237–2240.

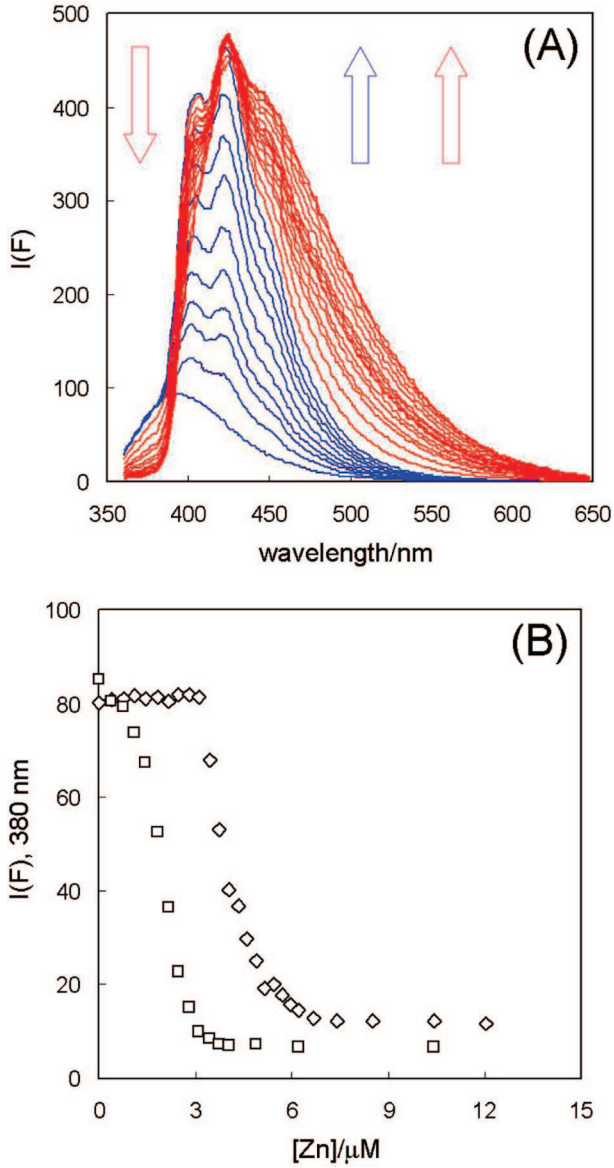

FIGURE 8. (A) Fluorescence spectra (λ_{ex} = 348 nm) of the mixture of **14** (2.0 μM) and **15** (2.0 μM) in MeCN (TBAP: 5 mM; DIPEA: 2 μM) with incremental addition of $Zn(ClO_4)_2$ (0−12 μM). Blue arrow and blue spectra follow the initial increase of fluorescence of **15** upon Zn^{2+} addition; red arrows and red spectra follow the delayed fluorescence modulation of **14** upon further Zn^{2+} addition. (B) □: fluorescence intensity of **14** at 380 nm (2 μM) with increasing [Zn]; ◇: fluorescence intensity of **14** and **15** at 380 nm (2 μM each) with increasing [Zn].

μM each immediately enhances the fluorescence of **15** (blue arrow in Figure 8A) before the occurrence of spectral change of **14** (red arrows in Figure 8A). The clear delay of spectral change of **14** in the presence of **15** (2 μM, Figure 8B) independently confirms our initial hypothesis that in MeCN, Zn^{2+} binds with dipicolyl group preferentially over bipy. Due to the dependence of apparent association constants and binding stoichiometries of dipicolylamino and bipy to Zn^{2+} on ligand concentration, solvent, and other factors, we prefer using the competitive binding experiment over comparing the apparent association constants of the two binding sites measured independently for evaluating the binding preference of zinc in a ditopic ligand.

Cyclic Voltammetry Studies. In a system of CHEF, a large fluorescence enhancement upon metal coordination is attributed

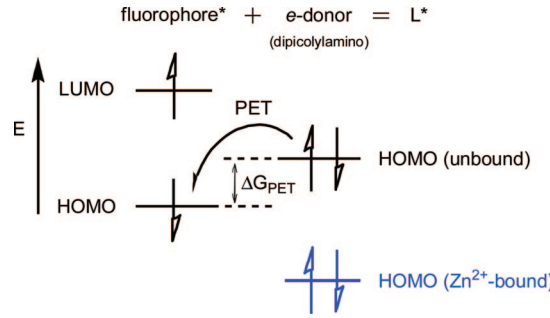

FIGURE 9. Frontier molecular orbitals of a PET system. The HOMO and LUMO of the excited fluorophore are on the left. The HOMO of the electron donor, in this study the dipicolylamino group, is on the right. When the dipicolylamino group is coordinated with Zn^{2+} (blue), the HOMO of the e-donor is lowered so that PET is not thermodynamically feasible.

to an efficient PET in the unbound ligand. Based on the Marcus equation, the efficiency (or rate) of PET is a function of the thermodynamic driving force (ΔG_{PET}) of PET.[73−76] The heightened fluorescence enhancements (Φ_{ZnL}/Φ_F, Table 1) of **9** and **10** over that of **7** and **8** upon coordinating the first Zn^{2+} are the results of increased ΔG_{PET} upon conversion from olefins to alkynes. In **7**−**10** where the excited fluorophores serve as electron acceptors in PET, as shown in Figure 9, the ΔG_{PET} is approximated as the energy gap between the highest occupied molecular orbitals (HOMOs) of the electron donors (in this study the dipicolylamino group) and the electron acceptors (various excited fluorophores). When the electron donors remain constant, the comparison of ΔG_{PET} in **7**−**10** can be made by comparing the HOMO levels of their fluorophores.[73,75]

$$\Delta G_{PET} = E_{ox(D)} - E_{red(A)} - E_{0,0} - w_p \quad (1)$$

$$E_{ox(A)} \approx E_{red(A)} + E_{0,0} \quad (2)$$

$$\Delta G_{PET} \approx E_{ox(D)} - E_{ox(A)} - w_p \quad (3)$$

$$\Delta G_{PET(A2)} - \Delta G_{PET(A1)} \approx E_{ox(A1)} - E_{ox(A2)} \quad (4)$$

The analysis of the Rehm−Weller equation (eq 1, all terms are in units of eV)[77] also concludes that the differences in ΔG_{PET} among **7**−**10** resulted primarily from the differences in the HOMO energy levels of their fluorophores. Oxidation (E_{ox}) and reduction (E_{red}) potentials of a molecule are proportional to its HOMO and LUMO energies, respectively. Therefore, the sum of E_{red} of a fluorophore and its excitation energy $E_{0,0}$ can be approximated as E_{ox} (eq 2). By substituting eq 2 into eq 1, eq 3 is obtained, which is the relationship that was reached by analyzing Figure 9 if w_p (the work term for the charge-separated state) is negligible. Therefore, when the electron donors are identical as in **7**−**10**, the difference in thermodynamic driving forces of PET ($\Delta\Delta G_{PET}$) of two ligands can be represented as the difference in E_{ox} (eq 4) of their fluorophores.

Cyclic voltammetry was applied to determine the E_{ox} of **7**−**14**. All compounds were oxidized irreversibly. The peaks

(73) Tanaka, K.; Miura, T.; Umezawa, N.; Urano, Y.; Kikuchi, K.; Higuchi, T.; Nagano, T. *J. Am. Chem. Soc.* **2001**, *123*, 2530–2536.
(74) Fahrni, C. J.; Yang, L.; VanDerveer, D. G. *J. Am. Chem. Soc.* **2003**, *125*, 3799–3812.
(75) Urano, Y.; Kamiya, M.; Kanda, K.; Ueno, T.; Hirose, K.; Nagano, T. *J. Am. Chem. Soc.* **2005**, *127*, 4888–4894.
(76) Ueno, S.; Tsukamoto, M.; Hirano, T.; Kikuchi, K.; Yamada, M. K.; Nishiyama, N.; Nagano, T.; Matuski, N.; Ikegaya, Y. *J. Cell. Biol.* **2002**, *158*, 215–220.
(77) Rehm, D.; Weller, A. *Isr. J. Chem.* **1970**, *8*, 259–271.

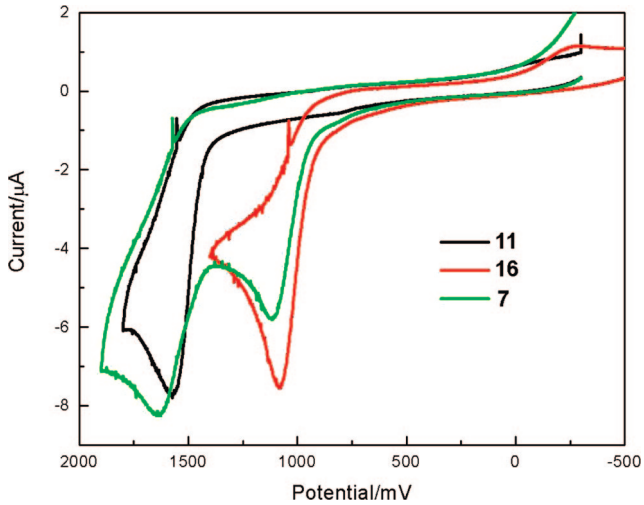

FIGURE 10. Cyclic voltammograms of **11**, **16**, and **7** in MeCN. Bu_4NPF_6 (0.1 M) was used as the supporting electrolyte. Working electrode: glassy carbon electrode; scan rate: 100 mV/s; reference electrode: Ag/AgCl.

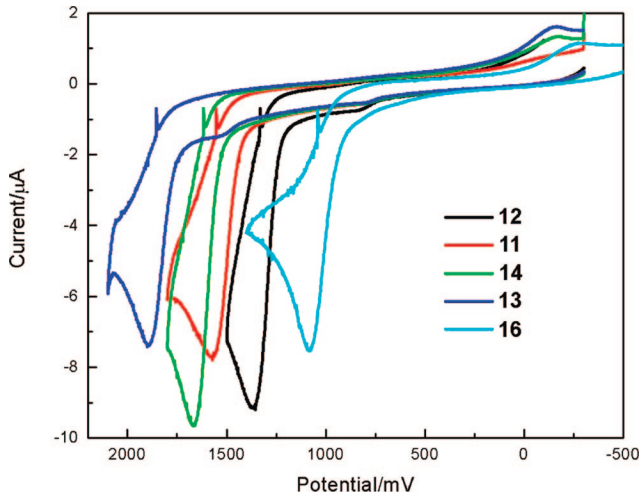

FIGURE 11. Cyclic voltammograms of **11**−**14** and **16** in MeCN. Bu_4NPF_6 (0.1 M) was used as the supporting electrolyte. Working electrode: glassy carbon electrode; scan rate: 100 mV/s; reference electrode: Ag/AgCl.

of **7** at 1636 mV and 1114 mV are assigned to the oxidation (anodic) peaks of the phenylvinyl-bipy fluorophore and the dipicolylamino group, respectively, based on the comparison with the cyclic voltammograms of monotopic ligands **11** and **16** (Figure 10). The higher oxidation potential of the fluorophore than that of the dipicolylamino group is consistent with the efficient PET observed in **7**. The observation of the two oxidation peaks of **7** supports our rationale where the HOMOs of e-donor and e-acceptor in an intramolecular PET system can be analyzed separately (Figure 9). The cyclic voltammograms of **8**−**10** are in the Supporting Information.

Monotopic ligands **11**−**14** and **16** were used for the comparison of oxidation potentials, hence HOMO levels, of different e-acceptors and an e-donor. Fluorophores **11**−**14** have oxidation potentials higher than that of **16**, *N*-methyldipicolylamine, which explains the thermodynamically favorable PET processes observed in **7**−**10** (Figure 11, anodic peak potentials are listed in Table 1). On the other hand, the alkynyl compounds (**13**, **14**) have lower HOMO levels than their vinyl analogs (**11**, **12**), which leads to more efficient PET processes in **9** and **10** than

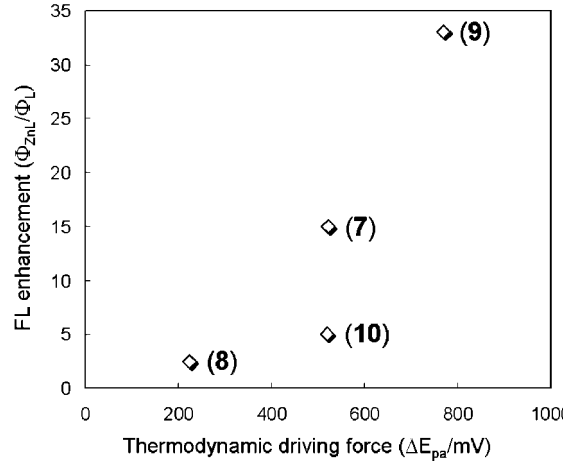

FIGURE 12. Correlation between fluorescence enhancements of ditopic ligands (**7**−**10**) upon coordination the first Zn^{2+} and thermodynamic driving force of PET (ΔE_{pa}) derived from the cyclic voltammograms of **7**−**10**.

those of their vinyl counterparts **7** and **8**, respectively. Consequently, upon Zn^{2+} coordination at the PET donor site dipicolylamino, **9** and **10** enjoy a greater extent of fluorescence restoration than that of **7** and **8**.

The fluorescence enhancements (Φ_{ZnL}/Φ_L) of heteroditopic ligands **7**−**10** over the first step coordination were plotted as a function of anodic potential differences (ΔE_{pa}) between the fluorophore and the dipicolylamino group (represented by **16**), which is considered as ΔG_{PET} in the unbound ligands. Evidently, fluorescence enhancement upon Zn^{2+} coordination increases with larger ΔG_{PET}. The substituent effect on the fluorescence quantum yields of arylvinyl-bipy and arylalkynyl-bipy systems is a topic of current study.

Conclusion

Photochemically stable fluorescent heteroditopic ligands **9** and **10** were prepared. The three coordination states in the presence or absence of Zn^{2+}, non-, mono-, and dicoordinated, are related to three distinct fluorescence states, OFF, ON at λ_1, and ON at λ_2. The binding stoichiometry of dipicolylamino and 2,2′-bipy to Zn^{2+} in MeCN were studied using Job's method of continuous variation and ITC, and were shown to be concentration dependent. The higher binding affinity of dipicolylamino to Zn^{2+} than that of 2,2′-bipy was demonstrated using a competitive binding experiment. Cyclic voltammetry studies indicated that the thermodynamic driving forces for PET (ΔG_{PET}) in unbound **9** and **10** are larger than those of free **7** and **8**, leading to larger fluorescence enhancements of **9** and **10** upon coordinating Zn^{2+}.

It was demonstrated in this study that fluorescence contrast between three coordination states of a fluorescent heteroditopic ligand can be rationally tuned by altering the structure of the fluorophore. Our dipicolylamino and 2,2′-bipy-based heteroditopic system also provides insight into binding stoichiometry of these commonly used bidentate and tridentate metal coordination ligands. The combination of Job's method and ITC may provide a wealth of information that would not be uncovered by either approach alone. The structure−function relationship pertaining to the coordination chemistry and photophysical processes in our heteroditopic systems will be applied in future rational design of fluorescent heteroditopic ligands tailor-made for specific applications.

Experimental Section

Representative procedures for preparing **9** and **10**.

Compound 22. NaH (60% in mineral oil, 4 mmol, 160 mg) was added at 0 °C to a solution of **21** (2.0 mmol, 356 mg) in dry dimethoxyethane (4.0 mL) in a flame-dried round-bottom flask. The suspension was stirred for 5 min. A solution of **20** (2.0 mmol, 641 mg) in dry dimethoxyethane (4.0 mL) was added dropwise to the flask while stirring at 0 °C. Following addition, the stirring was continued for 3 h while the temperature was brought to rt. The reaction mixture was then cooled to 0 °C before brine (2 mL) was added. The reaction mixture was stirred for another 5 min before partitioned between DCM and water. The aqueous layer was washed with DCM (50 mL × 3) and the organic portions were combined. The organic portions were dried over Na_2SO_4 followed by solvent removal under vacuum. The crude product was analyzed by TLC (silica, EtOAc, $R_f \approx 0.7$, an intensely blue fluorescent tailing spot). Compound **22** was isolated using silica chromatography eluted by EtOAc in DCM (gradient 0−30%). The isolated yield was 75%. ^{1}H NMR (300 MHz, $CDCl_3$): δ/ppm 8.76 (d, J = 1.8 Hz, 1H), 8.52 (s, 1H), 8.37 (d, J = 8.4 Hz, 1H), 8.30 (d, J = 8.4 Hz, 1H), 7.98 (dd, J = 2.4, 8.4 Hz, 1H), 7.65−7.49 (m, 5H), 7.41 (d, J = 8.4 Hz, 1H), 7.15 (d, J = 8.4 Hz, 1H), 5.84 (s, 1H), 4.19−4.04 (m, 4H), 2.41 (s, 3H); ^{13}C NMR (75 MHz, $CDCl_3$): δ/ppm 155.8, 153.5, 149.9, 148.3, 137.8, 137.6, 133.6, 132.7, 130.4, 127.1, 126.9, 126.6, 125.6, 120.8, 120.8, 103.7, 65.5, 29.9, 18.6; HRMS (ESI$^+$): calcd. ($C_{22}H_{20}N_2O_2$ + Na^+) 367.1422, found 367.1418.

Compound 23. A dry DCM solution (10 mL) of **22** (515 mg, 1.50 mmol) was added dropwise of a dry DCM solution (10 mL) of Br_2 (1.50 mmol, 77 μL) at 0 °C. The reaction mixture was stirred for another 3 h after addition was completed as the temperature of the reaction container rose to rt. The excess of Br_2 and solvent was removed carefully on a rotary evaporator at rt with $Na_2S_2O_3$ in the receiving flask to absorb Br_2. The residue from the bromination reaction was dissolved in anhydrous THF (5.0 mL) and cooled to 0 °C. ^{t}BuOK (6.0 mmol, 673 mg) was added and the reaction mixture was stirred for overnight. The reaction mixture was poured into icy water and product was extracted using DCM (50 mL × 3). The organic portions were combined and dried over Na_2SO_4 followed by solvent removal under vacuum. The crude product was analyzed by TLC (silica, EtOAc, $R_f \approx 0.8$). Compound **23** was isolated using silica chromatography eluted by EtOAc in DCM (gradient 0−15%). The yield was 25%. ^{1}H NMR (300 MHz, $CDCl_3$): δ/ppm 8.79 (d, J = 2.1 Hz, 1H), 8.52 (s, 1H), 8.37 (d, J = 8.1 Hz, 1H), 8.31 (d, J = 8.1 Hz, 1H), 7.92 (dd, J = 2.1, 8.1 Hz, 1H), 7.63 (dd, J = 2.1, 8.1 Hz, 1H), 7.59 (d, J = 8.1 Hz, 2H), 7.49 (d, J = 8.1 Hz, 2H), 5.84 (s,1H), 4.15−4.03 (m, 4H), 2.41 (s, 3H); ^{13}C NMR (75 MHz, $CDCl_3$): δ/ppm 155.2, 153.0, 151.7, 149.8, 139.4, 138.6, 137.6, 133.8, 131.8, 126.7, 123.6, 121.0, 120.1, 119.9, 103.3, 93.1, 87.1, 65.4, 18.5; HRMS (ESI$^+$): calcd. ($C_{22}H_{18}N_2O_2$ + H^+) 343.1446, found 343.1431.

Compound 24. Compound **23** (74 mg, 0.22 mmol) was dissolved in a mixed solvent (14 mL) of HCl (37%)/H_2O/THF = 1/6/7. The solution was stirred overnight before partitioned between basic brine (pH > 9) and EtOAc (3 × 50 mL). The organic portions were dried over Na_2SO_4 before concentrated under vacuum. The crude product was analyzed by TLC (silica, EtOAc, $R_f \approx 0.6$). The purity of the product judging by TLC and NMR (^{1}H and ^{13}C) spectra is sufficient for the next step. The yield was quantitative. ^{1}H NMR (300 MHz, $CDCl_3$): δ/ppm 10.04 (s, 1H), 8.82 (s, 1H), 8.52 (s, 1H), 8.41 (d, J = 8.1 Hz, 1H), 8.32 (d, J = 8.1 Hz, 1H), 7.95 (dd, J = 2.1, 8.4 Hz, 1H), 7.91 (d, J = 8.4 Hz, 2H), 7.72 (d, J = 8.4 Hz, 2H), 7.65 (dd, J = 2.1, 8.1 Hz, 1H), 2.41 (s, 3H); ^{13}C NMR (75 MHz, $CDCl_3$): δ/ppm 191.5, 155.8, 153.0, 151.9, 150.0, 139.7, 134.2, 137.7, 132.4, 129.8, 129.1, 121.2, 120.3, 119.3, 92.4, 90.6, 18.6; HRMS (ESI$^+$): calcd. ($C_{20}H_{14}N_2O$ + Na^+) 321.1004, found 321.1003.

Compound 9. Di-(2-picolyl)amine (38 μL, 0.21 mmol) was added dropwise to an anhydrous 1,2-dichloroethane (0.84 mL) solution of **24** (62 mg, 0.21 mmol). The mixture was stirred overnight before $NaBH(OAc)_3$ (89 mg, 0.42 mmol) was added. The mixture was stirred for another 5 h before the solvent was removed under vacuum. The residue was washed with basic brine (pH > 11) and extracted with DCM (3 × 50 mL). The organic portions were dried over K_2CO_3 before concentrated under vacuum. Compound **9** was isolated by alumina chromatography eluted by EtOAc in DCM (gradient 0−30%). The isolated yield was 73%. ^{1}H NMR (300 MHz, $CDCl_3$): δ/ppm 8.78 (s, 1H), 8.54−8.51 (m, 3H), 8.36 (d, J = 8.4 Hz, 1H), 8.30 (d, J = 8.4 Hz, 1H), 7.91 (dd, J = 1.8, 8.4 Hz, 1H), 7.71−7.42 (m, 9 H), 7.16 (t, J = 6.0 Hz, 2H), 3.82 (s, 4H), 3.71 (s,2H), 2.40 (s,3H); ^{13}C NMR (75 MHz, $CDCl_3$): δ/ppm 159.6, 155.0, 153.1, 151.6, 149.8, 149.1, 140.2, 139.3, 137.5, 136.5, 133.7, 131.8, 129.0, 122.9, 122.1, 121.4, 120.9, 120.1, 93.4, 86.5, 60.2, 58.4, 18.5; HRMS (ESI$^+$): calcd. ($C_{32}H_{27}N_5$ + Na^+) 504.2164, found 504.2161.

Acknowledgment. This work was supported by the Florida State University through a start-up fund, a New Investigator Research (NIR) grant from the James and Esther King Biomedical Research Program administered by the Florida Department of Health, and National Science Foundation (CHE 0809201). We thank Professor Kenneth Goldsby for the use of a Princeton Applied Research potentiostat (VersaStat), and Professor Mikhail Shatruk for helpful discussions and critical reading of the manuscript. We also thank the Institute of Molecular Biophysics at FSU for providing access to a VP-ITC microcalorimeter (Microcal) and Dr. Claudius Mundoma for technical assistance.

Supporting Information Available: Syntheses and characterization of new compounds, additional spectra, ITC data, and cyclic voltammograms. This material is available free of charge via Internet at http://pubs.acs.org.

JO8015083